# A MODEL FOR GENERATING RELATIVISTIC ELECTRONS IN THE EARTH'S INNER MAGNETOSPHERE BASED ON GYRORESONANT WAVE-PARTICLE INTERACTIONS

Danny Summers and Chun-yu Ma <sup>1</sup> Department of Mathematics and Statistics, Memorial University of Newfoundland,

St. John's, Newfoundland, A1C 5S7, Canada

Short title: RELATIVISTIC ELECTRONS IN THE INNER MAGNETOSPHERE

**Abstract.** During the recovery phase of a magnetic storm, fluxes of relativistic (> 1 MeV) electrons in the inner magnetosphere  $(3 \le L \le 6)$  increase to beyond pre-storm levels, reaching a peak about 4 days after the initiation of the storm. In order to account for the generation of these "killer electrons", a model is presented primarily based on stochastic acceleration of electrons by enhanced whistler-mode chorus. In terms of a quasi-linear formulation, a kinetic (Fokker-Planck) equation for the electron energy distribution is derived, comprising an energy diffusion coefficient based on gyroresonant electron-whistler-mode wave interaction and parallel wave propagation; a source term representing substorm-produced (lower energy) seed electrons; and a loss term representing electron precipitation due to pitch-angle scattering by whistler-mode waves and EMIC waves. Steady-state solutions for the electron energy distribution are constructed, and fitted to an empirically-derived relativistic Maxwellian distribution for the high energy "hard" electron population at geosynchronous orbit. If the average whistler amplitude is sufficiently large, for instance 75 pT - 400 pT, dependent on the values of the other model parameters, and assuming a background plasma density of  $N_0 = 10 \text{ cm}^{-3}$  outside the plasmasphere, then a good fit to the empirical distribution is obtained, and corresponds to a timescale for the formation of the high-energy steady state distribution of 3-5 days. For a lower representative value of the background plasma density,  $N_0 = 1 \text{ cm}^{-3}$ , smaller whistler amplitudes, in the range 13 – 72 pT, can produce the high-energy distribution in the required time frame of several days. It is concluded from the model calculations that the process of stochastic acceleration by gyroresonant electron-whistler-mode wave interaction, in conjunction with pitch-angle scattering by EMIC waves, constitutes a viable mechanism for generating "killer electrons" during geomagnetic storms. The mechanism is expected to be particularly effective for the class of small and moderate storms possessing a long-lasting recovery phase during which many substorms occur.

## 1. INTRODUCTION

It is well known that variations in the fluxes of relativistic electrons, of kinetic energies > 1 MeV, in the inner magnetosphere (3  $\leq L \leq 6$ ) are related to disturbed magnetospheric conditions commonly called "magnetic storms". Typically, for many storms the electron fluxes diminish rapidly during the main phase of the storm. The main phase depletion of relativistic electrons occurs in association with large negative values of the interplanetary magnetic field  $B_z$  and large sudden increases in the solar wind density and pressure [Paulikas and Blake, 1979; Blake et al., 1997]. Subsequently, during the recovery phase of the storm, fluxes increase to beyond pre-storm levels and peak about 4 days after the initiation of the storm [Paulikas and Blake, 1979; Baker et al., 1986, 1994a, 1997; Nagai, 1988; Li et al., 1997a; Reeves et al., 1998]. These enhancements in fluxes of relativistic electrons, which are colloquially referred to as "killer electrons", have become the subject of considerable attention by magnetospheric physicists. Not only do the enhancements constitute an intrinsically interesting physics problem in the near-Earth space, but they constitute a potentially serious hazard to satellites, space stations, and, conceivably, humans in space. In fact, satellite disfunctions ("anomalies") have been linked to the effects of relativistic electron increases |Baker| et al., 1994b, 1997, and the state of the radiation belt environment has become a major concern in space weather forecasting [e.g., Baker, 1998; Reeves, 1998a]. The region near geosynchronous (or geostationary) orbit,  $L \simeq 6.6$ , in the geographic equatorial plane, is of particular interest because it is the operating zone of many orbiting satellites. *Reeves* [1998b] has recently examined the relationship between relativistic electron enhancements at geosynchronous orbit and magnetic storms as measured by the  $D_{st}$ index. In particular, the 30 most intense relativistic electron events during 1992-1995 were examined, and it was found that every relativistic electron event was associated with a magnetic storm as indicated by the  $D_{st}$  index, though a small fraction (about 10%) of magnetic storms did occur with no increase in relativistic electron fluxes. Thus,

one conclusion from *Reeves*' [1998b] analysis is that intense solar wind conditions are necessary to generate strong relativistic electron enhancements. Nevertheless, despite the accumulated magnetic storm data from satellites over many years, including coordinated observations from the International Solar-Terrestrial Physics (ISTP) constellation of spacecraft and other multi-satellite missions [e.g., Baker et al., 1997; Reeves et al., 1998], there is, as vet, no accepted explanation for the generation of the relativistic electrons. Specifically, it is not known exactly how, where, or when the electrons are accelerated. Various energization mechanisms have been proposed, and most of these are reviewed by Li et al. [1997a]. It appears easier to explain the main phase depletion of energetic electrons than their subsequent recovery and enhancement. The drop in relativistic electron fluxes near geosynchronous orbit is partly due to adiabatic responses (conserving all three adiabatic invariants) to magnetic field decreases, as reflected in the reduction in  $D_{st}$  index [e.g., Kim and Chan, 1997]. Nevertheless, Li et al. [1997a] show that other physical mechanisms, including precipitation, must also contribute to the depletion. It has been suggested that radial diffusion [Schulz and Lanzerotti, 1974], invoked to explain the existence of the outer electron radiation belt itself, could also generate electrons of MeV energies in the inner magnetosphere. This mechanism, which involves inwardly transporting energetic electrons from a presumed source in the outer magnetosphere (in the tail), can produce such energies during relatively quiet periods [e.g., Selesnick and Blake, 1997a], although the process is too slow during active times [Li et al., 1997a; Blake et al., 1998]. Certain global recirculation processes, involving radial diffusion, have also been proposed to generate relativistic electrons e.g., Baker et al., 1986, 1989; Fujimoto and Nishida, 1990, though these have proved inadequate, as the transport rates are too slow. Sheldon et al. [1998] have recently identified the outer polar cusp region as a potential acceleration region of the magnetosphere and possible source of energetic electrons for the outer radiation belt, though further calculations are needed to evaluate the significance of the study. In another mechanism still to

be fully evaluated, *Rostoker et al.* [1998] and *Liu et al.* [1999] make the case that large-amplitude ULF pulsations have the potential to supply the energy necessary to create the enhanced relativistic electron fluxes. In a 3D global MHD simulation of the rapid rise of relativistic electron fluxes during the January 1997 magnetic cloud event, *Hudson et al.* [1999a, b] also found that ULF oscillations may play a role in energizing relativistic electrons, via a mechanism involving drift-resonant acceleration and radial transport.

It is becoming increasingly apparent that electrons are accelerated to relativistic (> 1 MeV) energies in situ in the inner magnetosphere [e.g., Blake et al., 1998]. Significant evidence in support of this conclusion is the observation by Selesnick and Blake [1997b] that the phase space density of electrons of greater than MeV energies peaks near L=4to L=5 during storms. As a result of substorm activity, electrons with energies up to  $\sim 300$  keV are injected near geosynchronous orbit [Cayton et al., 1989; Baker et al., 1989, 1998]. These electrons appear to form the source population for the relativistic electrons of greater than MeV energies that are subsequently observed. Summers et al. [1998, 1999] have shown that whistler-mode waves could provide an effective mechanism for accelerating electrons from energies near 100 keV to above 1 MeV in the region outside the plasmapause during the storm recovery phase. In a survey of potential wave modes for electron scattering and stochastic acceleration to relativistic energies during magnetic storms, Horne and Thorne [1998] concluded, in particular, that in low density regions of the magnetosphere where the electron gyrofrequency exceeds the electron plasma frequency, there are four potential wave modes that can resonate with electrons in the energy range 100 keV to a few MeV: the whistler, LO, RX, and Z modes. The concept of stochastic acceleration of electrons by whistler-mode waves in the magnetosphere has also been discussed by *Temerin et al.* [1994], Li et al. [1997a], Temerin [1998], and Roth et al. [1999]. It is the purpose of present paper to quantify the model presented qualitatively in Section 8 of Summers et al. [1998] for the stochastic

acceleration of relativistic electrons during geomagnetic storms. Essential ingredients in the model are the spatial regions within the inner magnetosphere  $3 \leq L \leq 9$  where enhanced whistler-mode chorus [Tsurutani and Smith, 1974, 1977; Koons and Roeder, 1990; Parrot and Gaye, 1994 and enhanced electromagnetic ion cyclotron (EMIC or L-mode) waves occur [Cornwall et al., 1970; Perraut et al., 1976; Jordanova et al., 1997; Kozyra et al., 1997]; see Figure 1. The aforementioned substorm-produced seed population of electrons in the energy range 100 keV to 300 keV have approximately circular drift paths within the region  $3 \leq L \leq 9$ , and consequently will traverse the regions of enhanced whistler-mode chorus and enhanced EMIC waves. Specifically, in this paper we shall model the acceleration of electrons during the storm recovery phase by means of second-order Fermi (or stochastic gyroresonant) acceleration by weak whistler-mode turbulence. In a standard quasi-linear formulation, we construct a kinetic equation for the evolution of the electron energy distribution function. The equation contains an energy diffusion coefficient due to resonant whistler-mode wave/electron interaction, and an electron loss term due to pitch-angle scattering by both the whistler-mode and EMIC waves. We should point out here that the data from the Solar, Anomalous, and Magnetospheric Particle Explorer (SAMPEX) satellite [Nakamura et al., 1995; Li et al., 1997a; Nakamura, 1998 show that bursty electron precipitation occurs as the electron flux increases during the storm recovery phase. Such precipitation, together with the existence of an abundant supply of storm-produced lower-energy seed electrons [Li et al., 1997a; Baker et al., 1998] are supportive of the model constructed in this paper. The model is presented in detail in Section 2, and numerical solutions are presented in Section 3. The solutions are compared with data on the electron energy distribution of high energy (300 – 2000 keV) electrons at geosynchronous orbit. We find that stochastic gyroresonant acceleration by whistler-mode waves can indeed accelerate substorm-produced seed electrons in the inner magnetosphere to generate high-energy electron spectra of the type observed, following continuous injection of seed electrons

over a timescale of several days. Specific predictions of the model depend, of course, on the values taken for the model parameters. In Section 4 we briefly assess our findings and state our conclusions.

## 2. MODEL

The region to which the model constructed in this paper applies is that part of the inner magnetosphere during storm-time that is illustrated in the idealized Figure 1, for  $3 \leq L \leq 9$ . This region contains an extensive subregion of whistler-mode chorus, a smaller but intense region of EMIC waves, and also contains the important geosynchronous-orbit region near L=6.6. Figure 1 is a simplified version of Figure 7 of Summers et al. [1998], which itself was constructed on the basis of observations and relevant theory [Cornwall et al., 1970; Perraut et al., 1976; Koons and Roeder, 1990; Parrot and Gaye, 1994; Tsurutani and Smith, 1974, 1977; Kozyra et al., 1997; Jordanova et al., 1997]. We assume that geomagnetic storm activity produces a seed population of electrons of energy  $\approx 100$  keV as a source for the region specified in Figure 1. We are not concerned in this paper with the precise means (transport, original source location, etc.) by which the source is supplied. According to standard particle drift theory [e.g., Wolf, 1995], the drift motion of "hot" (e.g., 100 keV) electrons close to the Earth is dominated by gradient drift, with the result that electrons execute approximately circular drift trajectories eastward about the Earth. Thus, the storm-supplied source electrons constitute a quasi-trapped population traversing the whistler-mode and EMIC wave subregions illustrated in Figure 1. While executing the eastward drift, the electrons gyrate about the field lines and 'bounce' between mirror points, during which time they also undergo both energy and pitch-angle diffusion, as a result of their interaction with the whistler-mode chorus and EMIC waves. We shall assume that the pitch-angle scattering rate is much greater than the energy diffusion rate (see Appendix A), so that the electron distribution will be nearly isotropic. Further,

#### Figure 1

we shall take account of pitch-angle diffusion of electrons into the loss-cone and their subsequent precipitation into the atmosphere, by characterizing their loss from the system by an escape time  $T_{esc}$ . The kinetic or Fokker-Planck equation describing the evolution in time t of the electron energy distribution function f(E, t) can be written as

$$\frac{\partial f}{\partial t} = \frac{\partial^2}{\partial E^2} \left( D(E)f \right) - \frac{\partial}{\partial E} \left[ \left( A(E) - |\dot{E}_L| \right) f \right] - \frac{f}{T_{esc}} + S(E, t), \tag{1}$$

where  $E = E_k/(m_e c^2) = \gamma - 1$  is the particle kinetic energy in units of the rest mass energy,  $\gamma = (1 - v^2/c^2)^{-1/2}$  is the Lorentz factor, v is the particle speed,  $m_e$  is the electron rest mass, and c is the speed of light; f(E,t)dE is the number of particles per unit volume in the interval dE; D(E) is the energy diffusion coefficient due to resonant interaction of the electrons with whistler-mode turbulence; A(E) is the systematic acceleration rate due to the whistler-mode turbulence;  $|E_L|$  is the energy loss rate due to processes not directly related to stochastic acceleration, namely, here assumed to be Coulomb collisions and synchrotron radiation;  $T_{esc}$  is the mean escape time of particles out of the system due to pitch-angle scattering by both whistler-mode and EMIC waves; and the source term S(E,t) represents the rate of particle injection into the inner magnetospheric region specified in Figure 1, as a result of storm activity. Equation (1) is not the standard form of Fokker-Planck equation employed in space physics, and so we give a brief account of its derivation in the Appendix. Detailed data on the whistler-mode chorus during storm-time are unfortunately not available. In fact, insufficient information is known about the energy spectrum of the turbulence in many space physics situations. While whistler-mode chorus emissions are normally considered to be discrete during geomagnetically quiet times [Anderson and Kurth, 1989], it is here assumed that during geomagnetic storms the concomitant, enhanced whistler-mode turbulence can be considered quasi-continuous. Specifically, a simplifying assumption is made that the whistler-mode turbulence is isotropic, homogeneous, stationary, and has a power-law spectral energy density distribution in wavenumber k, with spectral index

q; specifically, the spectral energy density is assumed to take the form,

$$W(k) = \frac{q-1}{k_{min}} \left(\frac{k_{min}}{k}\right)^q W_{tot}, \qquad W_{tot} = \int_{k_{min}}^{\infty} W(k) dk, \tag{2}$$

for wavenumbers greater than  $k_{min}$ , to be specified below. In accordance with the quasi-linear diffusion formulation adopted in this paper, the whistler-mode turbulence is weak, i.e., comprises small-amplitude magnetic and electric wave fields. Momentum diffusion coefficients corresponding to whistler-mode waves have been obtained by various authors. We calculate the Fokker-Planck coefficients D(E) and A(E) from (A8) using the whistler-mode diffusion coefficients  $D_p$  derived by Hamilton and Petrosian [1992] (for  $2 < q \leq 4$ ), and Schlickeiser [1997] (for 1 < q < 2) for parallel wave propagation. The results are

$$D(E) = D_0 \left[ E(E+2) \right]^{(q-1)/2} (E+1)^{-1},$$
(3)

$$A(E) = D_0 q \left[ E(E+2) \right]^{(q-3)/2}, \tag{4}$$

where

$$D_0 = \frac{\pi (q-1)^2}{q^2 (q^2 - 4)} \left(\frac{ck_{min}}{\Omega_e}\right)^{q-1} \alpha^2 R\Omega_e,\tag{5}$$

for  $2 < q \leq 4$ ;

$$D(E) = \mathcal{D}_0 \left[ E(E+2) \right]^{1/2} (E+1)^{-1}, \tag{6}$$

$$A(E) = 2\mathcal{D}_0 \left[ E(E+2) \right]^{-1/2}, \tag{7}$$

where

$$\mathcal{D}_0 = \frac{\pi(q-1)}{8} \left(\frac{ck_{min}}{\Omega_e}\right)^{q-1} \left(\frac{m_e}{m_p}\right)^{(2-q)/2} \alpha^{(2+q)/2} J_W R \Omega_e,\tag{8}$$

for 1 < q < 2.

In (3) – (8), the two dimensionless parameters R and  $\alpha$  are introduced; R is the ratio of turbulent energy  $W_{tot}$  to magnetic field energy,

$$R = 8\pi W_{tot} / B_0^2 = (\Delta B / B_0)^2, \qquad (9)$$

and

$$\alpha = \Omega_e^2 / \omega_{pe}^2 = (m_p / m_e) \beta_A^2, \tag{10}$$

where  $\Omega_e = eB_0/(m_ec)$  is the electron gyrofrequency, with  $B_0$  the ambient magnetic field strength and e the electron charge;  $\Delta B$  is the average whistler-mode wave amplitude;  $\omega_{pe} = (4\pi N_0 e^2/m_e)^{1/2}$  is the electron plasma frequency, with  $N_0$  the particle number density;  $J_W$  is a weakly varying function of E; and  $\beta_A = v_A/c$  where  $v_A = B_0/(4\pi N_0 m_p)^{1/2}$  is the Alfvén speed, with  $m_p$  the proton rest mass. The parameter  $\alpha$  defined in (10) is identical to the parameter  $\alpha$  used by *Summers et al.* [1998]. We note, in particular, as should indeed be the case, that since the kinetic energy variable E is dimensionless, the dimension of the diffusion coefficient D equals the dimension of the parameter  $D_0$  (or  $\mathcal{D}_0$ ) equals [time]<sup>-1</sup>. For definiteness, in (5) and (8) we set

$$k_{min} = \Omega_p / (c\beta_A), \tag{11}$$

[e.g., Hamilton and Petrosian, 1992], where  $\Omega_p = eB_0/(m_pc)$  is the proton gyrofrequency.

The energy loss term  $|\dot{E}_L|$ , in which we include losses due to Coulomb collisions and synchrotron radiation, can be expressed in the form

$$|\dot{E}_L| = 6 \times 10^{-13} N_0(E+1) [E(E+2)]^{-1/2} + 1.32 \times 10^{-9} B_0^2 E(E+2).$$
(12)

The first term on the right-hand side of the equation (12) is the energy loss rate due to Coulomb collisions, given by *Melrose* [1980], and the second term the energy loss rate due to synchrotron radiation, given by *Blumenthal and Gould* [1970]. In (12), the particle number density  $N_0$  is in cm<sup>-3</sup>, the magnetic field strength  $B_0$  is in gauss, and  $|\dot{E}_L|$  is in sec<sup>-1</sup>.

We note that there are potentially four influential parameters in the model: the parameter  $\alpha$  defined by (10), the spectral index q, the turbulent wave power parameter R, and the mean particle escape-time  $T_{esc}$ . The value of the parameter  $\alpha$  depends on the values taken for the particle density  $N_0$  and the ambient magnetic field strength  $B_0$ . We shall discuss  $T_{esc}$ , which we regard as an adjustable parameter, and the particle source function S below. The diffusion parameters  $D_0$  and  $\mathcal{D}_0$  occurring in expressions (3) and (6) for the diffusion coefficient D are measures of the rate of energy diffusion, and  $D_0^{-1}$ ,  $\mathcal{D}_0^{-1}$  are measures of the time scale for particle acceleration. Substituting the result (11) for  $k_{min}$  into equations (5) and (8), we find that  $D_0$  and  $\mathcal{D}_0$  are given by

$$D_0 = \frac{\pi (q-1)^2}{q^2 (q^2 - 4)} \left(\frac{m_e}{m_p}\right)^{q-3} \Omega_e R \beta_A^{5-q} = \frac{\pi (q-1)^2}{q^2 (q^2 - 4)} \left(\frac{m_e}{m_p}\right)^{(q-1)/2} \Omega_e R \alpha^{(5-q)/2},$$
(13)

for  $2 < q \leq 4$ ;

$$\mathcal{D}_{0} = \frac{\pi(q-1)}{8} \left(\frac{m_{p}}{m_{e}}\right) J_{W} \Omega_{e} R \beta_{A}^{3} = \frac{\pi(q-1)}{8} \left(\frac{m_{e}}{m_{p}}\right)^{1/2} J_{W} \Omega_{e} R \alpha^{3/2}, \tag{14}$$

for 1 < q < 2.

Corresponding to the Kolmogorov turbulent spectrum (q = 5/3), the function  $J_W$  is of order unity. As an idealized assumption, we regard the Kolmogorov spectrum as the representative spectrum over the range 1 < q < 2, and we henceforth set q = 5/3 and  $J_W = 1$  in (14).

Since, from (10), the parameter  $\alpha$  is inversely proportional to the particle number density  $N_0$ , it follows from (13) and (14) that  $D_0$  and  $\mathcal{D}_0$  increase as  $N_0$  decreases. This agrees with the conclusions of *Summers et al.* [1998] who found by constructing resonant diffusion curves in velocity space that energy diffusion becomes more pronounced with increasing  $\alpha$  (or decreasing  $N_0$ ). As expected, the values of  $D_0$  and  $\mathcal{D}_0$  also increase as the turbulent spectral energy density ratio R increases. Specifically, we find from (13) and (14) that  $D_0$  and  $\mathcal{D}_0$  depend on the plasma parameters  $N_0$  and  $B_0$ , and the wave amplitude  $\Delta B$  as follows:

$$D_0 \propto B_0^{(4-q)} (\Delta B)^2 / N_0^{(5-q)/2}$$
(15)

for  $2 < q \le 4;$ 

$$\mathcal{D}_0 \propto B_0^2 (\Delta B)^2 / N_0^{3/2}$$
 (16)

for 1 < q < 2.

In this paper, we set  $N_0 = 10 \text{ cm}^{-3}$  as the particle number density representative of the inner magnetosphere  $(3 \le L \le 9)$  outside the plasma sphere. It could be argued that such a value may be too high for the background plasma outside the plasmasphere. However, since from (15) and (16) it is clear that the acceleration process becomes more efficient as  $N_0$  decreases, we find it useful to adopt  $N_0 = 10 \text{ cm}^{-3}$  as a generic conservative value. We comment further on this assumption below. We use the equatorial (dipole) magnetic field value  $B_0 = 3.12 \times 10^{-5}/L^3$  T. Corresponding values of  $B_0$  and the above-defined parameters  $\alpha$  and  $\beta_A$  at the locations  $L = 3, 4, \dots, 9$  are given in Table 1. In Figure 2, we plot the energy diffusion parameter  $D_0$  (sec<sup>-1</sup>) as a function of the spectral index q in the range 2 < q < 4 at each of the locations L = 3, 4, 5. At each L-value, we calculate  $D_0$  for the specified wave amplitudes  $\Delta B = 75$  pT, 100 pT, 300 pT, and 1 nT (which correspond to the indicated values of R in the diagrams). Lines indicating the time scales  $D_0^{-1}$  for particle acceleration corresponding to 1 hour, 1/2 day, and 1 day are shown in each diagram. As can be observed from the curves in Figure 2, the value of  $D_0$  is particularly sensitive to the value of q as q approaches 2. In fact, formally from (13) we have the result  $D_0 \to \infty$ , as  $q \to 2$ , which is obviously undesirable physically, but which is a consequence of the quasi-linear diffusion formalism we have adopted in this paper. It is evident from Figure 2 that, at any given L-value, as the value of q decreases, the value of  $D_0$  increases, and hence the time scale for particle acceleration decreases. In addition, it can be observed that for a given value of q, as L decreases, the value of  $D_0$  likewise increases; this property also follows from relation (15). Thus, for q in the range 2 < q < 4, shorter acceleration times are favoured by smaller value of q, small values of L, and (of course) larger values of the wave amplitude  $\Delta B$ . Corresponding to the Kolmogorov spectrum (q = 5/3), we show in Figure 3 the diffusion parameter  $\mathcal{D}_0$  (sec<sup>-1</sup>) as a function of  $\Delta B$  (pT) at the locations L = 3, 4, 5. Again, it is clear from the figure that shorter acceleration times are favoured by smaller

Figure 2

Figure 3

values of L and larger values of  $\Delta B$ ; this property similarly follows from (16).

In Figure 4, we plot the diffusion coefficient D (sec<sup>-1</sup>) as a function of the particle kinetic energy E (MeV), as given by (3), (6), (13) and (14), for the fixed wave amplitude  $\Delta B = 1$  nT, and  $N_0 = 10$  cm<sup>-3</sup>. The curves are constructed for values of the spectral index q = 5/3, 2.5, 3, 3.5, and 4, at each of the locations, L = 3, 4, 5. The diffusion coefficient D is clearly an increasing function of energy E. In general, for a given value of E, though not at all values, D can also be seen to increase as q decreases.

According to the standard quasi-linear theory of resonant interaction of electrons with whistler-mode turbulence [e.g., *Melrose*, 1986], in order for electrons to resonate with whistlers, the condition,

$$\gamma \beta \ge (m_p/m_e)^{1/2} \beta_A \tag{17}$$

must be satisfied;  $\beta = v/c$  where v is the particle speed, c is the speed of light,  $\gamma$  is the Lorentz factor, and  $\beta_A = v_A/c$  is the Alfvén speed parameter defined above. Making use of relativistic relations given in (A6), we find that (17) can be expressed in the form

$$E(E+2) \ge (m_p/m_e)\beta_A^2 \tag{18}$$

which, in turn, by using the parameter  $\alpha$  defined in (10), can be reduced to

$$E \ge E_c,\tag{19}$$

where  $E_c$  is the critical energy given by

$$E_c = (1+\alpha)^{1/2} - 1.$$
(20)

The value of the parameter  $\alpha$  depends on the values of the particle number density  $N_0$  and magnetic field  $B_0$ . Values of the critical energy  $E_c$  are given in Table 1 at the locations  $L = 3, 4, \dots, 9$ , for  $N_0 = 10 \text{ cm}^{-3}$ ; the values for L = 3, 4, 5 correspond respectively to the energy cut-off values in the upper, middle, and lower diagrams in Figure 4.

Figure 4

#### Table 1

#### 3. NUMERICAL RESULTS

Prior to consideration of the solution of the kinetic equation (1) for the electron energy distribution function f(E, t), we must specify the source function S(E, t) which represents storm-produced seed electrons. We shall assume that the source function can be represented by a standard relativistic Maxwellian distribution, namely,

$$S = S_0[\mu/K_2(\mu)](E+1)[E(E+2)]^{1/2}e^{-\mu(E+1)}$$
(21)

where

$$\mu = m_e c^2 / (k_B T_s) \tag{22}$$

and  $T_s$  represents the temperature of the distribution;  $K_2(\mu)$  is a modified Bessel function of the second kind of argument  $\mu$ , and  $k_B$  is Boltzmann's constant. It can be shown that  $\int SdE = S_0$ , so that the parameter  $S_0$  represents the total number of source electrons per unit volume per unit time.

It is clearly important both to calibrate and test our model, as far as is possible at the present time, by making use of available observational data. The study by *Cayton et al.* [1989] appears best-suited to these purposes. *Cayton et al.* [1989] derived energy distribution functions from energetic (30 – 2000 keV) electron fluxes observed simultaneously by three satellites in geosynchronous orbit throughout the year 1986. It was found that the energetic electron population can be resolved into two distinct relativistic Maxwellian components, each parameterized by a temperature and a density: a lower energy (30 – 300 keV) "soft" electron distribution with temperature  $T_s \approx 25$ keV and number density  $N_s \approx 5 \times 10^{-3}$  cm<sup>-3</sup>; and a higher energy (300 – 2000 keV) "hard" electron distribution with temperature  $T_h \approx 200$  keV and number density  $N_h \approx 10^{-4}$ cm<sup>-3</sup>. The "soft" component is charaterized by intense substorm-related injections and by strong temporal variations. Accordingly, and in agreement with a suggested interpretation by *Cayton et al.* [1989], we shall regard this "soft" component as comprising the electron seed population. Thus, we shall identify the temperature  $T_s$  associated with the Maxwellian source distribution (21) - (22) as the aforementioned temperature of the "soft" electron component. *Cayton et al.* [1989] found that the value of  $T_h$  shows little change on the substorm (hourly) time scale, while  $N_h$  decreases during substorms. We shall regard the "hard" electron distribution as precisely the highly energetic ("killer") electron distribution that we are trying to model as a (steady-state) solution of the kinetic equation (1) with the steady Maxwellian source (21) – (22).

We solve equation (1) for the energetic electron distribution f(E, t) by the Crank-Nicholson implicit differencing scheme. The method is well suited to time-dependent Fokker-Planck equations, and we refer the reader to *Hamilton et al.* [1990] and *Park* and Petrosian [1996] for full details. Since we are concerned with the generation of a highly-energetic electron distribution, we assume that there are no such energetic particles initially, i.e.,

$$f(E,0) = 0,$$
  $E > E_s,$  (23)

where  $E_s = 1/\mu$  is the thermal energy associated with the source distribution (21) – (22). We further assume that, subject to continuous injection of the seed electrons (given by (21) – (22)), the evolving distribution maintains a maximum at  $E = E_s$  for all time, i.e., we take the inner boundary condition as

$$\frac{\partial f(E,t)}{\partial E} = 0, \qquad \qquad E = E_s. \tag{24}$$

Finally, for the outer boundary condition we require that the distribution function tend to zero for large values of E for all time, so we set

$$f(E,t) = 0,$$
  $E > E_0$  (25)

where  $E_0$  is a specified upper value of E (in practice, we fix  $E_0 = 2 \times 10^4$  MeV). Having constructed the evolving electron distribution subject to the above conditions, we thereby obtain the resulting steady-state distribution f(E) which we fit to a relativistic Maxwellian distribution, i.e., we carry out the linear fit,

$$\log_{10}\left[f(E)/\{(E+1)[E(E+2)]^{1/2}\}\right] \equiv a+bE,$$
(26)

with

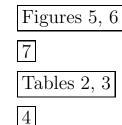
$$a = \log_{10} \left[ N_h \lambda e^{-\lambda} / K_2(\lambda) \right], \qquad b = -\lambda \log_{10} e, \qquad (27)$$

and

$$\lambda = m_e c^2 / (k_B T_h), \tag{28}$$

where  $T_h$  and  $N_h$  represent respectively the temperature and number density of the steady-state distribution (to be compared with the above values associated with the "hard" electron distribution); and  $K_2(\lambda)$  is a modified Bessel function of the second kind of argument  $\lambda$ . For a given steady-state solution, the parameters a and b are determined by a linear regression comprising a minimization of a chi-square goodness-of-fit merit function [*Press et al.*, 1992]. Having thus obtained values for a and b, we then calculate  $T_h$  and  $N_h$  from (27) and (28).

Representative numerical solutions of the model presented in this paper are shown in Figures 5, 6, and 7, with corresponding results given respectively in Tables 2, 3, and 4. In all cases we set the background number density  $N_0 = 10 \text{ cm}^{-3}$ , and the source electron temperature  $T_s = 25 \text{ keV}$  (giving  $\mu = 20.44 \text{ from } (22)$ ), the latter value being equal to the estimate by *Cayton et al.* [1989] for the temperature of the "soft" electron distribution. The scheme and rationale for setting the remaining parameters is as follows. Firstly, we set *L*, which fixes the value of the background magnetic field  $B_0$ . Secondly, we set the average wave-amplitude  $\Delta B$  and the spectral index q; these values are chosen to yield a value of the diffusion parameter  $D_0$  (or  $\mathcal{D}_0$ ) that is expected to produce a steady-state (equilibrium) distribution function after several days of source injection. Whistler-mode "chorus" wave amplitudes have been reported in the range 1 – 100 pT [*Burtis and Helliwell*, 1975], with *Parrot and Gaye* [1994] finding that during more intense periods of magnetic activity wave amplitudes can



approach  $\Delta B = 1$  nT. Amplitudes of whistlers associated mainly with hiss, with values of 100 pT or more, have also been reported by *Smith et al.* [1974] during a typical storm recovery phase. In Table 1, corresponding to a background number density of  $N_0 = 10 \text{ cm}^{-3}$ , we present the wave amplitudes  $\Delta B$  (pT) expected to yield a high energy "hard" electron distribution after a few days of seed electron injection as a result of substorm activity. These required amplitudes depend on the value of L and q (as well as  $N_0$ ). For q = 5/3, and for the inner region  $3 \le L \le 5$ , the values of  $\Delta B$  are in the range 75 - 400 pT, which are realistic though in the higher range of observations. As pointed out in Section 2, the process of gyroresonant stochastic acceleration becomes more efficient with decreasing background plasma density. While  $N_0 = 10 \text{ cm}^{-3}$  can be regarded as a representative value for the background plasma density outside the plasmasphere in certain conditions, it is also true that at other times  $N_0 = 1 \text{ cm}^{-3}$  is a more representative value. Using (15), we calculate that if we set  $N_0 = 1 \text{ cm}^{-3}$ , then, for  $3 \le L \le 5$ , the required  $\Delta B$ -values are in the range 13 – 72 pT, if q = 5/3, and in the range 35 – 316 pT, if  $2.5 \le q \le 3$ . Having set values for  $N_0, T_s, L, q$ , and  $\Delta B$ , we next specify the mean particle escape time  $T_{esc}$ . In fact, since a value for  $T_{esc}$  is not precisely known, we treat  $T_{esc}$  as an adjustable parameter and run the cases  $1/(D_0 T_{esc})$  $(\text{or } 1/(\mathcal{D}_0 T_{esc})) = 0, 1, 2, 5, 10.$  In Figure 5 (left) we show steady-state solutions for the electron energy distribution function f(E) for the case L = 3, q = 5/3,  $\Delta B = 75$ pT. The source strength  $S_0$  has been chosen so as to produce a model solution that best agrees with the "hard" electron distribution of *Cayton et al.* [1989]. In order to achieve this, for each steady-state solution the linear fit (26) - (28) to a relativistic Maxwellian distribution is carried out. The corresponding results are shown in Figure 5 (right) and Table 2. It is found that the temperature  $T_h$  associated with a particular steady-state solution, as given by the parameter b (or the slope of the constructed line), is largely determined by the value of  $T_{esc}$ , while the number density  $N_h$ , which is then given by the parameter a (or the vertical intercept of the line) is largely determined by

the value of  $S_0$ . The results in Table 2, for which  $S_0 = 1.5 \times 10^{-6} \text{ cm}^{-3} \text{sec}^{-1}$ , indicate a best agreement with the empirically-derived values of  $N_h \approx 10^{-4} \text{ cm}^{-3}$  and  $T_h = 200$ keV, when  $T_{esc} \approx 1/2$  day, the corresponding time for the formation of the steady-state solution being  $T_{EQ} \approx 4$  days. A precise, physically representative value for the mean particle escape time  $T_{esc}$  is difficult to determine *a priori* since  $T_{esc}$  relates to scattering losses of electrons due to both whistler-mode and EMIC waves. However, on the basis of estimates of timescales for strong diffusion scattering loss, it appears that  $T_{esc}$  is of the order of hours and so  $T_{esc} \approx 1/2$  day is not an unreasonable value. We relate  $T_{EQ}$  to the time taken after the initiation of a storm for fluxes of relativistic electrons to peak (see Section 1), which is observed to be several days. Thus, we favour solutions of the present model for which  $T_{EQ} = 1 - 5$  days, with  $T_{EQ} \approx 4$  days possibly the optimal value.

In Figure 6 and Table 3 we show the corresponding results for the case  $N_0 = 10$  cm<sup>-3</sup>, L = 6.6, q = 2.5,  $\Delta B = 800$  pT, while in Figure 7 and Table 4 we show the results for the case  $N_0 = 10$  cm<sup>-3</sup>, L = 5, q = 3,  $\Delta B = 1$  nT. As can be seen from the tables, for both these cases best agreement between the solutions and the "hard" electron distribution of *Cayton et al.* [1989] occurs when  $T_{esc} \approx 1/2$  day, and corresponds to a formation time  $T_{EQ} = 3 - 5$  days. If the background number density is taken to be  $N_0 = 1$  cm<sup>-3</sup>, the cases shown in Figures 6 and 7 correspond respectively to values for the wave amplitude  $\Delta B$  of 190 pT and 316 pT. Figures 6 and 7 correspond to cases of intense substorm activity during the storm recovery phase.

Taking into account the value of the wave amplitudes given in Table 2 corresponding to  $N_0 = 10 \text{ cm}^{-3}$ , and their converted values for the case  $N_0 = 1 \text{ cm}^{-3}$ , we re-iterate that the model solutions imply in particular that for a Kolmogorov turbulent wave spectrum, sustained whistler amplitudes in the physically realistic range 13 – 72 pT can generate a typical high energy "hard" electron distribution in the inner magnetosphere  $3 \leq L \leq 5$  within one or two days. It should also be noted that the model calculations show that the acceleration mechanism considered in this paper is not effective in the region  $7 \le L \le 9$  since the necessary values of the whistler amplitude would be too high (typically in excess of 1 nT). Thus, the model formulated herein has been shown to be a viable mechanism for accelerating electrons exactly in the inner region of the magnetosphere where the peak in electron phase space density of the highly energetic electrons is observed to occur [e.g., *Selesnick and Blake*, 1997b].

A requirement of the model presented here is enhanced whistler-mode chorus lasting for a period of at least one or two days. Geomagnetic conditions during which such a requirement is particularly well satisfied occur during the descending phase of the solar cycle when the Earth's magnetosphere can be impacted by a high-speed solar wind stream following a magnetic field build-up known as a Corotating Interaction Region (CIR). CIRs cause small and moderate magnetic storms, but not major storms. Since the Earth can be embedded in the associated high-speed stream for days to weeks there are substorms for days to weeks [*Tsurutani et al.*, 1995; *Kamide et al.*, 1998]. Thus, during this long-lasting recovery phase of the magnetic storm, there will be continuously enhanced wave activity, in the form of both whistler-mode chorus and EMIC waves, to drive the acceleration mechanism presented herein to generate the high energy (>1 MeV) electrons.

#### 4. CONCLUSIONS

In this paper, by means of quasi-linear theory and a test-particle approach, we have formulated the model kinetic equation (1) in which the acceleration mechanism is due to gyroresonant interaction between electrons and whistler-mode turbulence, corresponding to parallel wave propagation. The essential purpose of the study has been to apply equation (1) to the Earth's inner magnetosphere in order to test the hypothesis that storm-enhanced whistler-mode chorus can accelerate lower-energy substorm-produced seed electrons to relativistic (> 1 MeV) energies over a period of a few days. Our conclusions are as follows:

- 1. Based on the model calculations in this paper, it is entirely possible for enhanced whistler-mode chorus to generate the observed increases in relativistic (> 1 MeV) "killer" electrons during the storm recovery after a period of several days, so long as the waves are sufficiently strong. If  $N_0 = 10 \text{ cm}^{-3}$  is taken to be the background plasma number density outside the plasmasphere, the typical average wave-amplitudes required for a Kolmogorov spectrum are in the range  $\Delta B = 75 400 \text{ pT}$ , dependent on the location L. If  $N_0 = 1 \text{ cm}^{-3}$ , the required wave-amplitudes are in range 13 72 pT.
- 2. Energetic electron spectra of the model solutions do not follow a simple power law in energy. For certain sets of parameters, we find that solutions can be well fitted to the relativistic Maxwellian distribution empirically constructed by *Cayton et al.* [1989] to represent the higher energy (300 keV 2 MeV) "hard" electron population at geosynchronous orbit. We note the recent analysis by *Freeman et al.* [1998] of the November 3 4, 1993 storm, in which electrons from about 100 keV to 1.5 MeV were characterized by a power law spectrum. Evidently, optimal fitting of empirical electron spectra to power-law, Maxwellian, or other types of distribution can depend on the energy range prescribed and the event under consideration. In connection with electron power-law energy spectra, *Ma and Summers* [1998] have shown that such spectra can be produced by whistler-mode turbulence, although it is questionable whether the necessary conditions established in their theoretical study can be satisfied in the Earth's magnetosphere.
- 3. It is unlikely that any single physical mechanism of electron acceleration can fully account for relativistic electron enhancements occurring during the recovery phase of magnetic storms, not least because various types of energetic electron event have been observed [e.g., *Baker et al.*, 1997, 1998; *Reeves*, 1998b; *Reeves et*

al., 1998. Rapid energetic electron flux enhancements taking place over minutes have been associated with inductive electric fields [e.g., Li et al., 1993], while enhancements occurring over tens of minutes or a few hours have been linked to ULF pulsations [e.g., Rostoker et al., 1998; Liu et al., 1999]. The gradual acceleration process (occurring over a few days) formulated in this paper is not intended to apply to such energetic electron events which typically result from major storms. However, small and moderate magnetic storms associated with Corotating Interaction Regions (CIRs) characteristically have long recovery phases and attendant substorms for days to weeks [Tsurutani et al., 1995; Kamide et al., 1998]. Since these substorms produce enhanced whistler-mode chorus (and EMIC waves) over (at least) several days, the necessary conditions for the effectiveness of the mechanism presented in this paper are satisfied. Hence, for these types of storm, and possibly others, when average wave-amplitudes are sufficiently large, the present study shows that, in conjunction with pitch-angle scattering by EMIC waves, the mechanism of stochastic acceleration by whistler-mode turbulence is a serious candidate for explaining the generation of "killer electrons".

#### Appendix A: Derivation of the Fokker-Planck equation (1)

We consider energetic charged particles in a uniform magnetic field, with superimposed small-amplitude plasma waves of a given mode. The equation for the evolution of the particle distribution function  $\phi(p, t, \mu)$  due to gyroresonant interactions with the waves is

$$\frac{\partial \phi}{\partial t} = \frac{1}{p^2} \frac{\partial}{\partial p} \left( p^2 D_{pp} \frac{\partial \phi}{\partial p} \right) + \frac{1}{p^2} \frac{\partial}{\partial p} \left( p^2 D_{p\mu} \frac{\partial \phi}{\partial \mu} \right) + \frac{\partial}{\partial \mu} \left( D_{\mu p} \frac{\partial \phi}{\partial p} \right) 
+ \frac{\partial}{\partial \mu} \left( D_{\mu \mu} \frac{\partial \phi}{\partial \mu} \right) + \frac{1}{p^2} \frac{\partial}{\partial p} \left( p^2 \dot{\mathcal{E}}_L \phi \right) + Q(p, t).$$
(A1)

Equation (A1), called a kinetic or diffusion or Fokker-Planck equation, is derived by expanding a collisionless Boltzmann equation for the particle distribution function

to second order in perturbed quantities, and ensemble-averaging over the statistical properties of the plasma waves in accordance with quasi-linear theory. Among the early authors to carry out this procedure were Kennel and Engelmann [1966], Hall and Sturrock [1967], and Lerche [1968]; see also Melrose [1980], Schlickeiser [1989], and Steinacker and Miller [1992], and references therein. In (A1), p is the relativistic unit momentum given by  $p = \gamma v/c$ , where v is the particle speed, and  $\gamma = (1 - v^2/c^2)^{-1/2}$  is the Lorentz factor, with c the speed of light; t is time;  $\mu$  is the cosine of the pitch angle;  $\mathcal{E}_L$  is an energy loss term due to processes not directly associated with gyro-resonant wave-particle interactions; and Q(p,t) is a source term. The Fokker-Planck or diffusion coefficients  $D_{pp}, D_{p\mu}, D_{\mu p}$ , and  $D_{\mu \mu}$  depend on the properties of the wave turbulence, viz., the wave mode and polarization, the angle of wave propagation to the ambient magnetic field, and the power spectrum, including the ratio of the turbulent wave energy to the background magnetic energy. These coefficients have been given both in general form, and specific form, for various particular wave modes, by a number of authors, e.g., Melrose [1980], Schlickeiser [1989], Steinacker and Miller [1992], and Hamilton and Petrosian [1992]. It is not necessary here to derive equation (A1), which requires considerable algebra, or to provide general expressions for the coefficients  $D_{pp}, D_{p\mu} = D_{\mu p}$ , and  $D_{\mu \mu}$ . We shall assume that the rate of pitch-angle scattering is much larger than the rate of energy diffusion (and the rate of the particle escape from the system). Such an assumption is reasonable based on an analysis of time scales associated with resonant interaction of electrons with whistler-mode waves, e.g., see Melrose [1980] and the discussion by Hamilton and Petrosian [1992]. Equivalently, defining the time scales  $T_{\mu\mu} = D_{\mu\mu}^{-1}$ ,  $T_{\mu p} = p D_{\mu p}^{-1}$ ,  $T_{pp} = p^2 D_{pp}^{-1}$ , and the escape time  $T_{esc}$ , we assume that  $T_{\mu\mu} \ll T_{pp}$ ,  $T_{\mu\mu} \ll T_{\mu p}$ , and  $T_{\mu\mu} \ll T_{esc}$ . Then the particle distribution function can be assumed to be isotropic, and the pitch angle can be eliminated from the problem by integrating (A1) with respect to  $\mu$  [e.g., see Schlickeiser, 1989; Steinacker

and Miller, 1992]. Writing

$$F(p,t) = \int_{-1}^{1} \phi(p,t,\mu) d\mu,$$
 (A2)

and representing the scattering loss of particles by pitch angle diffusion by means of a loss term  $-F(p,t)/T_{esc}$ , the equation (A1) thus becomes

$$\frac{\partial F(p,t)}{\partial t} = \frac{1}{p^2} \frac{\partial}{\partial p} \left( p^2 D_p(p) \frac{\partial F(p,t)}{\partial p} \right) + \frac{1}{p^2} \frac{\partial}{\partial p} \left( p^2 \dot{\mathcal{E}}_L(p) F(p,t) \right) \\
- \frac{F(p,t)}{T_{esc}} + \frac{1}{2} Q(p,t),$$
(A3)

where the momentum diffusion coefficient  $D_p(p)$  has been formed by averaging with respect to  $\mu$ .

We now change the momentum variable p to the kinetic energy variable  $E = \gamma - 1$ in equation (A3). We write

$$f(E,t)dE = 4\pi p^2 F(p,t)dp, \qquad (A4)$$

$$\frac{\partial}{\partial p} = \frac{dE}{dp} \frac{\partial}{\partial E},\tag{A5}$$

and make note of the following simple relativistic relations:

$$p = \gamma \beta, \beta = v/c, p^2 = E(E+2), \gamma = (1+p^2)^{1/2},$$
  

$$pdp = (E+1)dE, \beta dp = dE, \beta = [E(E+2)]^{1/2}(E+1)^{-1}.$$
 (A6)

Then, after straightforward manipulation, equation (A3) can be expressed in the form,

$$\frac{\partial}{\partial t} \left( f(E,t) \right) = \frac{\partial^2}{\partial E^2} \left[ D(E)f(E,t) \right] - \frac{\partial}{\partial E} \left[ \left( A(E) - |\dot{E}_L| \right) f(E,t) \right] - \frac{f(E,t)}{T_{esc}} + S(E,t), \tag{A7}$$

where

$$D(E) = \beta^2 D_p(p),$$
  

$$A(E) = \frac{1}{p^2} \frac{d}{dp} \left( p^2 \beta D_p(p) \right),$$
  

$$|\dot{E}_L| = \beta \dot{\mathcal{E}}_L(p),$$

$$S(E,t) = \frac{2\pi p^2}{\beta}Q(p,t).$$
(A8)

The form of equation (A7) is actually the Fokker-Planck form of equation for a particle distribution function as originally presented by *Chandrasekhar* [1943] for particles in stochastic motion. Stochastic acceleration of electrons in solar flares has been treated using different versions of (A7), e.g., see *Ramaty* [1979], *Petrosian* [1994], and *Park et al.* [1997].

#### Acknowledgments.

This work is supported by the Natural Sciences and Engineering Research Council of Canada under Grant A-0621. Additional support is acknowledged from the Dean of Science, Memorial University of Newfoundland, as well as NSF Grant ATM 97 29021 and NASA Grant NAG5 4680. Part of this paper was written when D. Summers was Visiting Professor at the Radio Atmospheric Science Center, Kyoto University, Japan. It is a pleasure to acknowledge H. Matsumoto of Kyoto University for his generous hospitality and stimulating scientific discussions. We are also grateful to R. B. Horne and B. T. Tsurutani for helpful comments.

## References

- Anderson, R. R., and W. S. Kurth, Discrete electromagnetic emissions in planetary magnetospheres, *Plasma Waves and Instabilities at Comets and in Magnetospheres*, *Geophys. Monog. 53*, edited by B. T. Tsurutani and H. Oya, p. 81, A.G.U., Washington, D.C., 1989.
- Baker, D. N., J. B. Blake, R. W. Klebesadel, and P. R. Higbie, Highly relativistic electrons in the Earth's outer magnetosphere, I. Lifetimes and temporal history 1979-1984, J. Geophys. Res., 91, 4265, 1986.
- Baker, D. N., J. B. Blake, L. B. Callis, R. Belian, and T. E. Cayton, Relativistic electrons near geostationary orbit: Evidence for internal magnetospheric acceleration, *Geophys. Res. Lett.*, 16, 559, 1989.
- Baker, D. N., J. B. Blake, L. B. Callis, J. R. Cummings, D. Hovestadt, S. Kanekal, B. Blecker,
  R. A. Mewaldt, and R. D. Zwickl, Relativistic electron acceleration and decay time scales in the inner and outer radiation belts: SAMPEX, *Geophys. Res. Lett.*, 21, 409, 1994a.
- Baker, D. N., S. Kanekal, J. B. Blake, B. Klecker, and G. Rostoker, Satellite anomalies linked to electron increase in the magnetosphere, *Eos, Trans.*, AGU, 75, 402, 1994b.
- Baker, D. N., X. Li, N. Turner, J. H. Allen, L. F. Bargatze, J. B. Blake, R. B. Sheldon, H.
  E. Spence, R. D. Belian, G. D. Reeves, S. G. Kanekal, B. Klecker, R. P. Lepping,
  K. Ogilvie, R. A. Mewaldt, T. Onsager, H. J. Singer, and G. Rostoker, Recurrent
  geomagnetic storms and relativistic electron enhancements in the outer magnetosphere:
  ISTP coordinated measurements, J. Geophys. Res., 102, 14141, 1997.
- Baker, D. N., Radiation belt models and forecasts, Eos, Trans., AGU, 79, W93, 1998.
- Baker, D. N., T. I. Pulkkinen, X. Li, S. G. Kanekal, J. B. Blake, R. S. Selesnick, M. G. Henderson, G. D. Reeves, H. E. Spence, and G. Rostoker, Coronal mass ejections, magnetic clouds, and relativistic electron events: ISTP, J. Geophys. Res., 103, 17279, 1998.

- Blake, J. B., D. N. Baker, N. Turner, K. W. Ogilvie, and R. P. Lepping, Correlation of changes in the outer-zone relativistic-electron population with upstream solar wind and magnetic field measurements, *Geophys. Res. Lett.*, 24, 927, 1997.
- Blake, J. B., R. S. Selesnick, J. F. Fennell, M. Grande, and C. H. Perry, A comparison of the injection parameters of relativistic electrons and ring current ions as observed by CRRES, *Eos, Trans.*, AGU, 79, W99, 1998.
- Blumenthal, G. R., and R. J. Gould, Bremsstrahlung, synchrotron radiation, and Compton scattering of high-energy electrons traversing dilute gases, *Rev. Mod. Phys.*, 42, 237, 1970.
- Burtis, W. J., and R. A. Helliwell, Magnetospheric chorus: amplitude and growth rate, J. Geophys. Res., 80, 3265, 1975.
- Cayton, T. E., R. D. Belian, S. P. Gary, T. A. Fritz, and D. N. Baker, Energetic electron components at geosynchronous orbit, *Geophys. Res. Lett.*, 16, 147, 1989.
- Chandrasekhar, S., Stochastic problems in physics and astronomy, *Rev. Mod. Phys.*, 15, 1, 1943.
- Cornwall, J. M., F. V. Coroniti, and R. M. Thorne, Turbulent loss of ring current protons, J. Geophys. Res., , 75, 4699, 1970.
- Freeman, J. W., T. P. O'Brien, A. A. Chan, and R. A. Wolf, Energetic electrons at geostationary orbit during the November 3 – 4, 1993 storm: Spatial/temporal morphology, characterization by a power law spectrum, and representation by an artificial neural network, J. Geophys. Res., 103, 26251, 1998.
- Fujimoto, M. and A. Nishida, Energization and anisotropization if energetic electrons in the Earth's radiation belt by the recirculation process, J. Geophys. Res., 95, 4265, 1990.
- Hall, D. E., and P. A. Sturrock, Diffusion, scattering, and acceleration of particles by stochastic electromagnetic fields, *Phys. Fluids*, 10, 2620, 1967.
- Hamilton, R. J., E. T. Lu, and V. Petrosian, Numerical solution of the time-dependent kinetic equation for electrons in magnetized plasma, Astrophys. J., 354, 726, 1990.

- Hamilton, R. J., and V. Petrosian, Stochastic acceleration of electrons. I. Effects of collisions in solar flares, Astrophys. J., 398, 350, 1992.
- Horne, R. B., and R. M. Thorne, Potential wave modes for electron scattering and stochastic acceleration to relativistic energies during magnetic storms, *Geophys. Res. Lett.*, 25, 3011, 1998.
- Hudson, M. K., S. R. Elkington, J. G. Lyon, and C. C. Goodrich, Increase in relativistic electron flux in the inner magnetosphere: ULF wave mode structure, Adv. Space Res., in press, 1999a.
- Hudson, M. K., S. R. Elkington, J. G. Lyon, C. C. Goodrich, and T. J. Rosenberg, Simulation of radiation belt dynamics driven by solar wind variations, *Sun-Earth Plasma Connections, Geophys. Monog. 109*, edited by J. L. Burch, S. K. Antiochos, R. L. Carovillano, p. 171, A.G.U., Washington, 1999b.
- Jordanova, V. K., J. U. Kozyra, A. F. Nagy, and G. V. Khazanov, Kinetic model of the ring current-atmosphere interactions, J. Geophys. Res., 102, 14279, 1997.
- Kamide, Y., W. Baumjohann, I. A. Daglis, W. D. Gonzalez, M. Grande, J. A. Joselyn, R. L. McPherron, J. L. Phillips, E. G. D. Reeves, G. Rostoker, A. S. Sharma, H. J. Singer, B. T. Tsurutani, and V. M. Vasyliunas, Current understanding of magnetic storms: Storm-substorm relationships, J. Geophys. Res., 103, 17705, 1998.
- Kennel, C. F., and F. Engelmann, Velocity space diffusion from weak plasma turbulence in a magnetic field, *Phys. Fluids*, 9, 2377, 1966.
- Kim, H.-J., and A. A. Chan, Fully adiabatic changes in storm time relativistic electron fluxes, J. Geophys. Res., 102, 22107, 1997.
- Koons, H. C., and J. L. Roeder, A survey of equatorial magnetospheric wave activity between 5 and 8 R<sub>E</sub>, Planet. Space Sci., 38, 1335, 1990.
- Kozyra, J. U., V. K. Jordanova, R. B. Horne, and R. M. Thorne, Modeling of the contribution of electromagnetic ion cyclotron (EMIC) waves to storm ring current erosion,

Magnetic Storms. Geophys. Monog. 98, edited by B. T. Tsurutani et al., p. 187, A.G.U., Washington, D.C., 1997.

- Lerche, I., Quasilinear theory of resonant diffusion in a magneto-active relativistic plasma, *Phys. Fluids*, 11, 1720, 1968.
- Li, X., I. Roth, M. Temerin, J. R. Wygant, M. K. Hudson, and J. B. Blake, Simulation of the prompt energization and transport of radiation belt particles during the March 24 , 1991 SSC, *Geophys. Res. Lett.*, 20, 2423, 1993.
- Li, X., D. N. Baker, M. Temerin, T. E. Cayton, E. G. D. Reeves, R. A. Christensen, J. B. Blake, M. D. Looper, R. Nakamura, and S. G. Kanekal, Multi-satellite observations of the outer zone electron variation during the November 3-4, 1993, magnetic storm, J. Geophys. Res., 102, 14123, 1997a.
- Li, X., D. N. Baker, M. Temerin, D. Larson, R. P. Lin, G. D. Reeves, M. D. Looper, S. G. Kanekal, and R. A. Mewadt, Are energetic electrons in the solar wind the source of the outer radiation belt? *Geophys. Res. Lett.*, 24, 923, 1997b.
- Liu, W. W., G. Rostoker, and D. N. Baker, Internal acceleration of relativistic electrons by large-amplitude ULF pulsations, J. Geophys. Res., 104, 17391, 1999.
- Ma, C.-Y., and D. Summers, Formation of power-law energy spectra in space plasmas by stochastic acceleration due to whistler-mode waves, *Geophys. Res. Lett.*, 25, 4099, 1998.
- Melrose, D. B., Plasma Astrophysics, Vol. II: Nonthermal Processes in Diffuse Magnetized Plasmas, Gordon and Breach, New York, 1980.
- Melrose, D. B., Instabilities in Space and Laboratory Plasmas, Cambridge University Press, New York, 1986.
- Nagai, T., Space weather forecast: Prediction of relativistic electron intensity at synchronous orbit, *Geophys. Res. Lett.*, 15, 425, 1988.
- Nakamura, R., D. N. Baker, J. B. Blake, S. Kanekal, B. Klecker, and D. Hovestadt, Relativistic electron precipitation enhancements near the outer edge of the radiation belt, *Geophys. Res. Lett.*, 22, 1129, 1995.

- Nakamura, R., Precipitation of electrons of the outer radiation belt during geomagnetic storm, Eos, Trans., AGU, 79, W100, 1998.
- Park, B. T., and V. Petrosian, Fokker-Planck equations of stochastic acceleration: a study of numerical methods, Astrophys. J. (Supp.), 103, 255, 1996.
- Park, B. T., V. Petrosian, and R. A. Schwartz, Stochastic acceleration and photon emission in electron-dominated solar flares, Astrophys. J., 489, 358, 1997.
- Parrot, M., and C. A. Gaye, A statistical survey of ELF waves in a geostationary orbit, Geophys. Res. Lett., 21, 2463, 1994.
- Paulikas, G. A., and J. B. Blake, Effects of the solar wind on magnetospheric dynamics: Energetic electrons at the synchronous orbit, in *Quantitative Modeling of magnetospheric Processes, Geophys. Monog. 21*, edited by W. P. Olsen, p. 180, A.G.U., Washington, D.C., 1979.
- Perraut, S., R. Gendrin, and A. Roux, Amplification of ion-cyclotron waves for various typical radial profiles of magnetospheric parameters, J. Atmos. Terr. Phys., 38, 1191, 1976.
- Petrosian, V., Acceleration of electrons in solar flares, in *High-energy Solar Phenomena, AIP Conf. Proc. 294*, edited by J.M. Ryan, and W.T. Vestrand, p. 162, AIP, New York, 1994.
- Press, W. H., B. P. Flannery, S. A. Teukolsky, and W. T. Vetterling, Numerical Recipes in C: The Art of Scientific Computing, Cambridge University Press, New York, 1992.
- Ramaty, R., Energetic particles in solar flares, in *Particle Acceleration Mechanisms in Astrophysics*, edited by J. Arons, C. Max, and C. Mckee, p. 135, AIP Conf. Proc. 56, New York, 1979.
- Reeves, G. D., Relativistic electrons, space weather, and the next solar maximum, *Eos, Trans.*, *AGU*, 79, W93, 1998a.
- Reeves, G. D., Relativistic electrons and magnetic storms: 1992-1995, Geophys. Res. Lett., 25, 1817, 1998b.

- Reeves, G. D., R. H. W. Friedel, R. D. Belian, M. M. Meier, M. G. Henderson, T. Onsager,
  H. J. Singer, D. N. Baker, X. Li, and J. B. Blake, The relativistic electron response at geosynchronous orbit during the January 1997 magnetic storm, J. Geophys. Res., 103, 17559, 1998.
- Rostoker, G., S. Skone, and D. N. Baker, On the origin of relativistic electrons in the magnetosphere associated with some geomagnetic storms, *Geophys. Res. Lett.*, 25, 3701, 1998.
- Roth, I., M. Temerin, and M. K. Hudson, Resonant enhancement of relativistic electron fluxes during geomagnetically active periods, Ann. Geophysicae, 17, 631, 1999.
- Schlickeiser, R., Cosmic-ray transport and acceleration. I. Derivation of the kinetic equation and application to cosmic rays in static cold media, Astrophys. J., 336, 243, 1989.
- Schlickeiser, R., γ-ray evidence for galactic in-situ electron acceleration, Astron. Astrophys., 319, L5, 1997.
- Schulz, M., and L. Lanzerotti, Particle Diffusion in the Radiation Belts, Springer, New York, 1974.
- Selesnick, R. S., and J. B. Blake, Dynamics of the outer radiation belt, Geophys. Res. Lett., 24, 1347, 1997a.
- Selesnick, R. S., and J. B. Blake, Observations of relativistic electron acceleration in the outer radiation belt, *Eos, Trans.*, AGU, SM31E-10, Dec., 1997b.
- Sheldon, R. B., H. E. Spence, J. D. Sullivan, T. A. Fritz, and J. Chen, The discovery of trapped energetic electrons in the outer cusp, *Geophys. Res. Lett.*, 25, 1825, 1998.
- Smith, E. J., A. M. A. Frandsen, B. T. Tsurutani, R. M. Thorne, and K. W. Chan, Plasmaspheric hiss intensity variations during magnetic storms, J. Geophys. Res., 79, 2507, 1974.
- Steinacker, J., and J. A. Miller, Stochastic gyroresonant electron acceleration in a low-beta plasma. I. Interaction with parallel transverse cold plasma waves, Astrophys. J., 393, 764, 1992.

- Summers, D., R. M. Thorne, and F. Xiao, Relativistic theory of wave-particle resonant diffusion with application to electron acceleration in the magnetosphere, J. Geophys. Res., 103, 20487, 1998.
- Summers, D., R. M. Thorne, and F. Xiao, A model for stochastic acceleration of electrons during geomagnetic storms, Adv. Space Res., in press, 1999.
- Temerin, M., I. Roth, M. K. Hudson, and J. R. Wygant, New paradigm for the transport and energization of radiation belt particles, *Eos, Trans.*, AGU, 75, 538, 1994.
- Temerin, M. A., Heating of radiation belt electrons by whistler waves, Eos, Trans., AGU, 79, W100, 1998.
- Tsurutani, B. T., and E. J. Smith, Postmidnight chorus: A substorm phenomenon, J. Geophys. Res., 79, 118, 1974.
- Tsurutani, B. T., and E. J. Smith, Two types of magnetospheric ELF chorus and their substorm dependences, J. Geophys. Res., 82, 5112, 1977.
- Tsurutani, B. T., W. D. Gonzalez, A. L. C. Gonzalez, F. Tang, J. K. Arballo, and M. Okada, Interplanetary origin of geomagnetic activity in the declining phase of the solar cycle, *J. Geophys. Res.*, 100, 21717, 1995.
- Walt, M., Introduction to Geomagnetically Trapped Radiation, Cambridge University Press, New York, 1994.
- Wolf, R. A., Magnetospheric configuration, in *Introduction to Space Physics*, M. K. Kivelson and C. T. Russell, Cambridge University Press, New York, p. 317, 1995.

<sup>1</sup> On leave from Purple Mountain Observatory, Chinese Academy of Sciences, Nanjing, P.R. China.

Danny Summers and Chun-yu Ma, Department of Mathematics and Statistics, Memorial University of Newfoundland, St. John's, Newfoundland, A1C 5S7, Canada (e-mail: dsummers@math.mun.ca, cyma@math.mun.ca)

Received ??? ??, 1999; revised ??? ??, 1999; accepted ??? ??, 1999.

Submitted to Journal of Geophysical Research , 1999.

Figure 1. (Left) Schematic view in the magnetic equatorial plane of the approximately circular (projected) drift path of relativistic electrons in the inner magnetosphere. During storms these energetic electrons drift (eastward) through regions of enhanced whistler-mode chorus and enhanced electromagnetic ion cyclotron (EMIC) waves. (Right) Representation of the gyration about magnetic field lines and the bounce motion of energetic electrons as they execute the approximately circular drift path shown in (a).

Figure 2. Diffusion coefficient  $D_0$  given by (13) as a function of the turbulence spectral index q, for 2 < q < 4. The upper, middle, and lower diagrams correspond respectively to the locations L = 3, 4, 5. The background particle number density  $N_0 = 10 \text{ cm}^{-3}$ . In each diagram, curves are shown corresponding to the four indicated values of the wave power R (given by (9)) which correspond to the respective average wave amplitudes  $\Delta B = 75$ pT, 100 pT, 300 pT, 1 nT.

Figure 3. Diffusion coefficient  $\mathcal{D}_0$  given by (14) as a function of the average wave amplitude  $\Delta B$  (pT), at each of the locations L = 3, 4, 5. The turbulence spectral index q = 5/3, the parameter  $J_W = 1$ , and the background particle number density  $N_0 = 10$ cm<sup>-3</sup>.

Figure 4. Diffusion coefficient D given by (3), (6), (13), (14) as a function of the particle kinetic energy E, for the average wave amplitude  $\Delta B = 1$  nT, and the indicated values of the spectral index q. The upper, middle, and lower diagrams correspond respectively to the locations L = 3, 4, 5. The background particle number density  $N_0 = 10$  cm<sup>-3</sup>. Figure 5. (Left) Steady state solutions f(E) to the kinetic equation (1) for the electron energy distribution function, for the indicated values of  $1/(\mathcal{D}_0 T_{esc})$ , corresponding to different mean particle escape times. The diffusion coefficient and systematic acceleration rate are given by (6) and (7), with the diffusion parameter  $\mathcal{D}_0$  defined by (14); q = 5/3,  $J_W = 1, L = 3, \Delta B = 75 \text{ pT}, N_0 = 10 \text{ cm}^{-3}, \text{ and } \mathcal{D}_0 = 7.8 \times 10^{-6} \text{ sec}^{-1}$ . The particle source function is given by (21), with  $S_0 = 1.5 \times 10^{-6} \text{ cm}^{-3} \text{ sec}^{-1}$  and  $\mu = 20.44$ . (Right) Corresponding re-scaled plots of the solution curves on the left, for comparison with relativistic Maxwellian energy distribution functions. The dashed lines represent best fits with Maxwellian distributions in accordance with the results given in Table 2.

Figure 6. (Left) Steady state solutions f(E) to the kinetic equation (1) for the electron energy distribution function, for the indicated values of  $1/(D_0 T_{esc})$ , corresponding to different mean particle escape times. The diffusion coefficient and systematic acceleration rate are given by (3) and (4), with the diffusion parameter  $D_0$  defined by (13); q = 2.5, L = 6.6,  $\Delta B = 800$  pT,  $N_0 = 10$  cm<sup>-3</sup>, and  $D_0 = 7.2 \times 10^{-6}$  sec<sup>-1</sup>. The particle source function is given by (21), with  $S_0 = 1.4 \times 10^{-9}$  cm<sup>-3</sup> sec<sup>-1</sup> and  $\mu = 20.44$ . (Right) Corresponding re-scaled plots of the solution curves on the left, for comparison with relativistic Maxwellian energy distribution functions. The dashed lines represent best fits with Maxwellian distributions in accordance with the results given in Table 3.

Figure 7. (Left) As in Figure 6 (Left), but for the parameters q = 3, L = 5,  $\Delta B = 1$  nT,  $N_0 = 10 \text{ cm}^{-3}$ , and  $D_0 = 6.5 \times 10^{-6} \text{ sec}^{-1}$ . The particle source function is given by (21), with  $S_0 = 1.9 \times 10^{-8} \text{ cm}^{-3} \text{ sec}^{-1}$  and  $\mu = 20.44$ . (Right) Corresponding re-scaled plots of the solution curves on the left, for comparison with relativistic Maxwellian energy distribution functions. The dashed lines represent best fits with Maxwellian distributions in accordance with the results given in Table 4.

**Table 1.** Values of the magnetic field  $B_0$  (10<sup>-7</sup> T), the parameters  $\alpha$  and  $\beta_A$  given by (10), and the critical energy  $E_c$  (keV) given by (20), corresponding to the locations  $L = 3, 4, \dots, 9$ ; the background particle number density is  $N_0 = 10 \text{ cm}^{-3}$ . Also given, corresponding to the indicated values of the spectral index q, are typical values of the average wave amplitude  $\Delta B$  (pT) and the associated values of the diffusion parameters  $\mathcal{D}_0$  and  $D_0$  in sec<sup>-1</sup>(×10<sup>-6</sup>) required to produce a high energy "hard" electron distribution after several days of sub-storm particle injection.

					q = 5/3		q = 2.5		q = 3.0	
L	$B_0$	$\alpha$	$\beta_A$	$E_c$	$\Delta B$	$\mathcal{D}_0$	$\Delta B$	$D_0$	$\Delta B$	$D_0$
3	11.6	1.31	0.027	267	75	7.8	150	8.6	500	7.6
4	4.85	0.23	0.011	57	200	9.8	300	9.3	700	6.2
5	2.50	0.061	0.006	15	400	10	400	6.1	1000	6.5
6	1.44	0.019	0.0032	4.8	600	7.3	600	5.7	1200	5.3
7	0.91	0.0081	0.0021	2.1	900	7.0	800	5.4	1500	5.4
8	0.61	0.0036	0.0014	0.9	1400	7.5	1200	6.6	1800	5.1
9	0.43	0.0018	0.001	0.5	2000	7.6	1500	6.1	2200	5.4

Table 2. Results associated with the steady-state solutions shown in Figure 5. Each line of the table corresponds to the particular value of  $T_{esc}$  (the mean particle escape time) indicated. Each solution is fitted to a relativistic Maxwellian distribution by means of the linear fit (26) in which the parameters a and b yield values for the number density  $N_h$  and temperature  $T_h$  of the distribution;  $\chi^2$  measures the goodness-of-fit. The time taken for the steady-state (equilibrium) distribution to form is  $T_{EQ}$ .

$1/(\mathcal{D}_0 T_{esc})$	$T_{esc}$ (day)	a	$b(\times 10^{-3})$	$\chi^2$	$N_h( imes 10^{-4}) \ { m cm}^{-3}$	$T_h \; (\mathrm{keV})$	$T_{EQ}$ (day)
0	$\infty$	-2.25	-1.01	3.95	160	430	10
1	1.5	-3.41	-1.11	0.30	8.9	390	8
2	0.75	-3.76	-1.40	0.32	2.4	310	5
5	0.3	-3.88	-2.17	0.11	0.8	190	3
10	0.15	-3.85	-3.08	0.046	0.4	140	1

$1/(D_0 T_{esc})$	$T_{esc}$ (day)	a	$b(\times 10^{-3})$	$\chi^2$	$N_h(\times 10^{-4}) \ {\rm cm}^{-3}$	$T_h \; (\mathrm{keV})$	$T_{EQ}$ (day)
0	$\infty$	-3.47	-0.58	0.77	3.8	750	11
1	1.6	-3.56	-1.5	0.052	3.2	280	8
2	0.8	-3.74	-2.0	0.034	1.2	220	5
5	0.4	-4.00	-2.9	0.010	0.32	150	3
10	0.2	-4.17	-3.9	0.034	0.13	110	1

**Table 3.** As for Table 2, except the results are associated with the steady-state solutions inFigure 6.

$1/(D_0 T_{esc})$	$T_{esc}$ (day)	a	$b(\times 10^{-3})$	$\chi^2$	$N_h(\times 10^{-4}) \ {\rm cm}^{-3}$	$T_h \; (\mathrm{keV})$	$T_{EQ}$ (day)
0	$\infty$	-4.00	-0.22	21	140	2000	12
1	1.8	-3.90	-1.1	1.8	3.3	410	9
2	0.9	-4.02	-1.5	0.88	1.2	290	5
5	0.45	-4.19	-2.3	0.31	0.32	190	3
10	0.2	-4.30	-3.3	0.12	0.12	130	1

**Table 4.** As for Table 2, except the results are associated with the steady-state solutions inFigure 7.

